

# On The Use of the Equivalent Source Method for Nearfield Acoustic Holography

Marcos Eduardo Vieira Pinho  
[mpinho@fem.unicamp.br](mailto:mpinho@fem.unicamp.br)

José Roberto de França Arruda  
[arruda@fem.unicamp.br](mailto:arruda@fem.unicamp.br)

Departamento de Mecânica Computacional - DMC  
Faculdade de Engenharia Mecânica  
Universidade Estadual de Campinas - UNICAMP  
C.P. 6122 – 13083-970 – Campinas - SP

*Abstract. The mapping of sound pressure fields radiated from vibrating structures has an important role on the characterization of noise sources. Among the methods generally used to obtain a radiation map, Nearfield Acoustic Holography (NAH), which is based on the Fourier acoustics theory, is the most common. NAH is a powerful tool for pressure field estimation. However, it has several restrictions involving the necessary experimental arrangement. In this paper, a preliminary comparison between conventional planar NAH and the Equivalent Source Method (ESM) is presented. ESM consists in replacing the vibrating surface (source) with a set of elementary acoustic sources (monopoles) which gives rise to the same sound field, in some sense, as the original source. Differently from standard NAH, ESM is shown to be independent of the coordinate system, and can be used for arbitrary measurement grids. Some simple simulated cases are presented. The robustness of both methods is investigated by adding noise to numerically simulated data. Comparisons between the two methods are shown for different distances of the measurement plane relative to the source plane, both for backward and forward propagation. Finally, an experimental validation that uses both methods is presented. The advantages and disadvantages of each method are discussed.*

**Keywords.** *vibroacoustics, acoustic holography, inverse problem, pressure mapping*

## 1. Introduction

The legislation in many countries has been more strict regarding targets of noise emitted by industrial products, in order to provide a higher comfort level and an improved quality of life. This is especially true for automobiles, aircraft and residential systems (e.g., air conditioners and refrigerators), where, sometimes, the comfort level is as important as functionality. Among the factors determining the comfort level, mechanical vibration and acoustic noise are two of the main nuisances that affect the human perception. Therefore, noise and vibration analysis is becoming a key factor in product design. The acoustic holography technique can be utilized in the reconstruction of an acoustic source in order to fully map the radiated pressure field, thus obtaining a complete and detailed vibroacoustic characterization of the vibrating structure and identifying the main noise sources. In this way, either an intervention in the source or an active or passive control application in the radiated acoustic field can be realized in a more effective way.

The noise source reconstruction problem is usually associated with the Nearfield Acoustic Holography (NAH) technique. Based upon Fourier acoustics, it consists in obtaining the three dimensional sound field from pressure measurement near to the surface that radiates the sound. The NAH technique presents good results for sources with simple, or separated, geometry. However, it has limitations in case of arbitrarily shaped sources, which correspond to the kind of source generally found in industrial applications.

The Boundary Element Method (BEM) is a numerical technique employed for radiation problems and, by itself or associated to structural models based on the Finite Element Method (FEM), allows obtaining solutions for complex vibroacoustic problems (Schuhmacher, 2000). Inverse numerical models can be used to characterize acoustic sources. Although numerical methods are well accepted, the computational time can still be prohibitively high, mainly for higher frequencies. Therefore, alternative methods for the characterization of acoustic fields are an attractive subject. The acoustic holography by Elementary Source Method (ESM) can be situated in this context.

The ESM consists of replacing the vibrating structure by a set of elementary acoustical sources, usually lying in the interior of the structure, which, together, give rise to an acoustic field matching the field outside the structure. Differently from standard NAH, the acoustic holography technique by ESM allows to estimate the pressure field anywhere, independently of the noise source geometry, the

measurement grid or the coordinate system utilized. The inverse radiation model by ESM frequently results in a discrete, ill-conditioned problem. Therefore, regularization tools such as Tikhonov's are used in order to improve the reconstruction of the acoustic source strength.

In this paper, the ESM is analyzed for sets with different number of elementary sources. Varying the distance of the receiving array from the source, a comparative analysis between ESM and NAH is performed. In order to make the radiation model more representative, random error was added to the simulated data, and the robustness of both acoustical holography methods, ESM and NAH, were evaluated.

Finally, a real-life acoustic radiation problem is presented, where a vibrating plate is used as a noise source. The Tikhonov regularization is evaluated and the reconstructions by ESM and NAH for this experimental case are compared. The advantages and disadvantages of each acoustical holography method are discussed. Recommendations are made concerning the use of ESM or NAH to achieve the reconstruction of a radiated acoustic field.

## 2. Acoustical holography by the Elementary Source Method (ESM)

The ESM theory, shown to be equivalent to the Helmholtz-integral formulation by Koopman et al. (1986), is based on Eq.(1), which expresses the acoustic field at a point  $r_1$  due to a sound source located at position  $r_2$ :

$$P(r_1, r_2) = j\rho_0\omega \int_V q(r_2)g(r_1, r_2)dV(r_2), \quad (1)$$

where  $j = \sqrt{-1}$ ,  $\rho_0$  is the density of the fluid,  $\omega$  is the angular frequency and  $q$  is the source strength. For  $N$  elementary sources,  $q(r_{2_n})$ ,  $n = 1, \dots, N$ , the previous equation can be rewritten in the discretized form, for a discrete point locate at  $r_{1_m}$ :

$$P(r_{1_m}) = \sum_{n=1}^N \frac{j\omega\rho_0}{4\pi} \frac{q(r_{2_n})}{d(r_{1_m}, r_{2_n})} e^{-jkd(r_{1_m}, r_{2_n})}, \quad m = 1, \dots, M, \quad (2)$$

where  $d$  is the distance from the point-source to the field point and  $k$  is the wavenumber. Suppose that, for the sound field reconstruction,  $M$  measurements are necessary, and assume that the system of equations is either square or overdetermined, i.e.,  $M \geq N$ . The general problem to be considered can be rewritten in the discrete matrix form:

$$[A]_{(M \times N)} \{Q\}_{(N \times 1)} = \{P\}_{(M \times 1)}, \quad (3)$$

where  $[A]$  is a complex transfer matrix and  $\{p\}$  is a vector of measured of sound pressures. The unknown source strength vector  $\{Q\}$ , that produces the measured  $\{p\}$ , is obtained by solving the inverse problem using the following equation:

$$Q = [A]^H [A] + \beta [I]^{-1} [A]^H \{P\}, \quad (4)$$

where  $[I]$  is the identity matrix,  $\beta$  is the regularization parameter and  $^H$  indicates the complex conjugate transpose of a matrix. For  $\beta$  null, the solution is the least-squares solution, and, for  $\beta \neq 0$ , the solution is said to be regularized (Tikhonov).

## 3. Simulation case

In order to explore the main features of the ESM and compare the results with the results obtained by NAH, a series of simulation analyses was undertaken, in which the volume velocities were reconstructed for a vibrating, simply supported plate mounted on a baffle. This kind of sound source is used for its simple geometry, which allows the plane NAH technique to be applied. The plate characteristics were: Young' modulus = 207 GPa, thickness = 1.433mm, mass density = 7800 kg/m<sup>3</sup>, Poisson's coefficient = 0.3, and dimensions 0.4m x 0.5m.

### 3.1 ESM: number of elementary sources

One of the main challenges of the ESM is determining an optimal source configuration, as discussed by Barbosa (2001) and Magalhães (2002). As the integration on the right-side of Eq.(1) is replaced by the finite summation in Eq.(2), the increase of the number of elementary sources number,  $N$ , will reduce the error caused by this approximation, as shown by Koopman et al. (1986). However, a larger number of sources increase the dimension of matrix  $[A]$  to be inverted, and the system can become ill conditioned. In order to obtain a better understanding of this problem, the ESM behavior was analyzed for four source configurations, respectively with 24, 100, 200, and 315 sources, spaced apart from one another in a symmetrical arrangement, as shown in Fig.(1), where the red circles indicate the positions of sources in the plane  $z = 0$ , and the black crosses indicate the point fields, in the plane  $z_0 = 4\text{cm}$ .

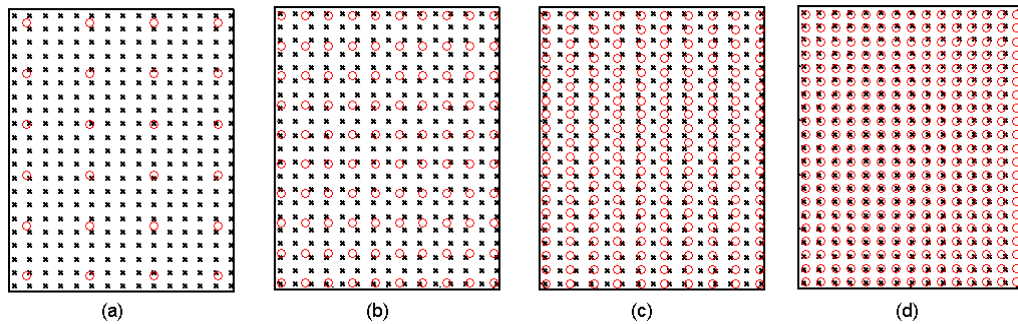


Figure 1. Four sets of elementary sources, indicated on red circles at  $z = 0$ , and the measurement grid, indicated by black crosses at  $z = 4\text{cm}$  for: (a) 24-source model; (b) 100-source model; (c) 200-source model; (d) 315-source model.

For each of these systems, the condition number was calculated for each frequency, and results are shown in Fig.(2).

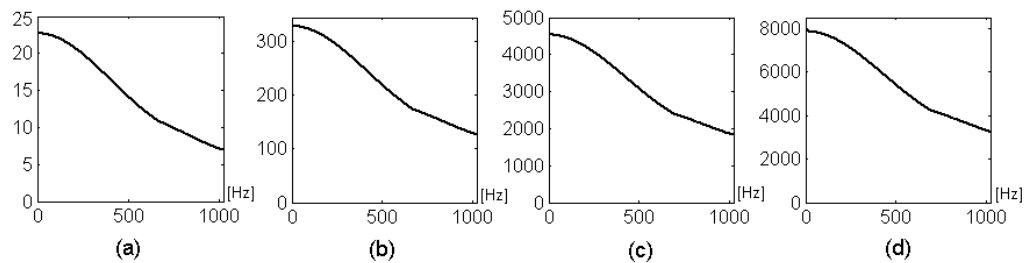


Figure 2. Condition number for the four sets of elementary sources. (a) 24-source model; (b) 100-source model; (c) 200-source model; (d) 315-source model.

The curves shown depict the variation in the condition number for a range of modeled sources. It is clear that the matrix of transfer function becomes ill conditioned as the number of sources increase. This result was expected, since increasing the number of sources increase the size of matrix  $[A]$ . For the four models analyzed, a pressure field parallel and with the same size as the vibrating plate was estimated in the planes  $z = 1\text{cm}$  and  $z = 8\text{cm}$ , which were compared with the pressure field obtained analytically. Fig.(3) shows the relative error of the estimated acoustic field.

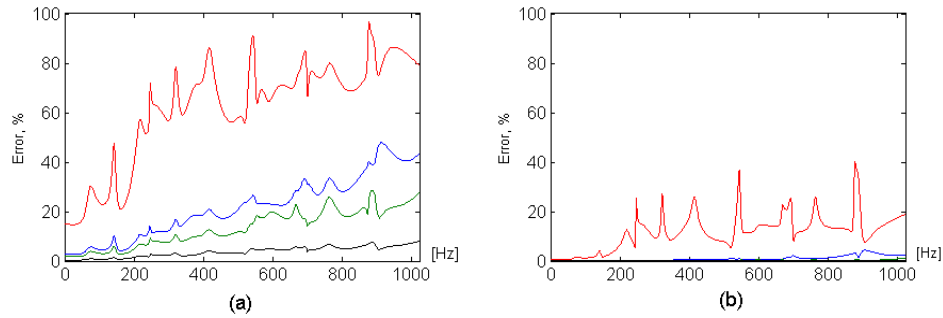


Figure 3. Relative error of ESM 24-source model (red), 100-source model (blue), 200-source model (green), and 315-source model (black), for the measurement grid at  $z_0 = 4\text{cm}$  and for two estimated planes. (a)  $z = 1\text{cm}$ ; (b)  $z = 8\text{cm}$

By comparing the results it can be noted that increasing the number of sources leads to more accurate results, although the condition number of matrix  $[A]$  increases. Note that, in the backpropagation case ( $z = 1\text{cm}$ ), the 24-source model could not obtain good results. In the forward propagation case ( $z = 8\text{cm}$ ), it must be highlighted that the results reached by the 100, 200 and 315-source models, presented relative errors that are negligible.

### 3.2 ESM: distance between the measurement plane and the acoustic source plane

For the NAH technique application, it is necessary that the input plane be near to the source, in order to assure the presence of evanescent waves in the measured data, as shown by Williams (1999). In order to evaluate the influence of this distance for the ESM reconstruction, the method was analyzed for four distances  $z_0$  of the receiving array to the source plane:  $z_0 = 1\text{cm}$ ,  $z_0 = 4\text{cm}$ ,  $z_0 = 8\text{cm}$ , and  $z_0 = 12\text{cm}$ . The 200-source model, shown in Fig.(1), was used. The conditioning number curves for each system are presented in Fig.(4).

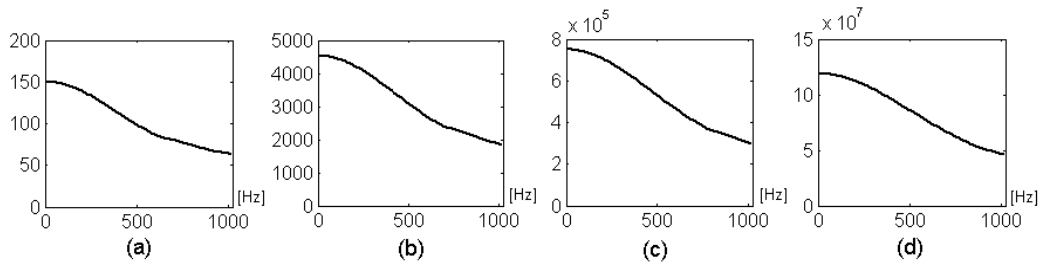


Figure 4. Conditioning number curves for a 200-source model, for four distances between the receiving array and the source. (a)  $z_0 = 1\text{cm}$ ; (b)  $z_0 = 4\text{cm}$ ; (c)  $z_0 = 8\text{cm}$ ; (d)  $z_0 = 12\text{cm}$ .

It can be noticed that the conditioning number becomes worse as the distance from the input plane to the source plane becomes larger, as shown by Nelson (2000,b). For the four models analyzed, a pressure field parallel and with the same size of the vibrating plate was estimated in three planes of interest:  $z = 2\text{cm}$ ,  $z = 6\text{cm}$  and  $z = 10\text{cm}$ , and compared with the analytical solution. In an analogous form, for the same input data, the NAH modified by using a Regressive Fourier Series (Arruda, 1997) was applied in order to obtain the reconstructed pressure field. The results obtained with both acoustical holography methods are compared and the relative error of each case is presented.

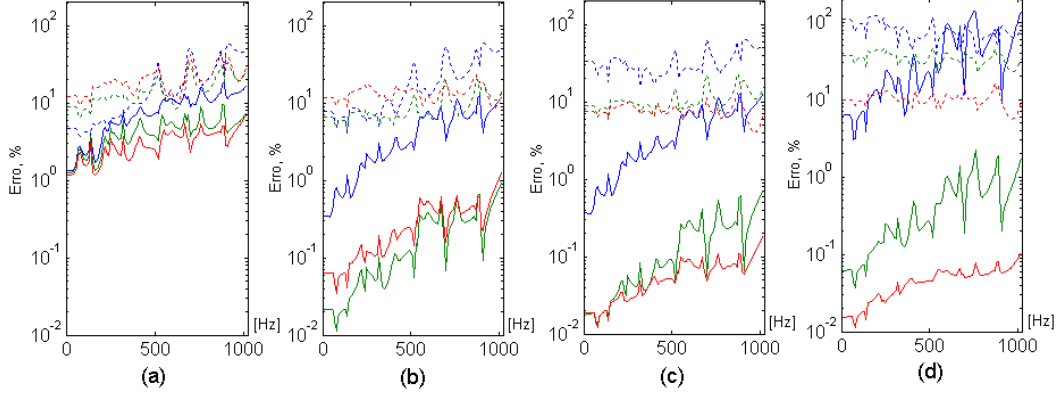


Figure 5. Relative error of ESM (solid) and NAH (dotted) results for three distances between the reconstruction plane and the source,  $z = 2\text{cm}$  (blue),  $z = 6\text{cm}$  (green), and  $z = 10\text{cm}$  (red) for four distances between the receiving array and the source: (a)  $z_0 = 1\text{cm}$ , (b)  $z_0 = 4\text{cm}$ , (c)  $z_0 = 8\text{cm}$ , (d)  $z_0 = 12\text{cm}$ .

From the error plots shown in Fig.(5), it is clear that, in this case study, the ESM results are more accurate than the NAH solution. By comparing the results obtained for the two different methods, one can recognize an important aspect: while the NAH reconstruction accuracy increases as the receiving array is closer to the source, the ESM estimation is either indifferent or even improves as the input plane moves away from the source. For both acoustic holography methods, it could be noticed clearly that moving the reconstruction plane away from the source improves the solution achieved. The excellent accuracy of ESM for some pressure planes reconstructed (at  $z = 6\text{cm}$  and  $z = 10\text{cm}$ ) is also noted with relative errors of less than 1% (both back propagation and forward propagation). Furthermore, another interesting aspect observed in ESM is the indifference with relation to the condition number of matrix  $[A]$ . Except for  $z_0 = 1\text{cm}$ , all other cases presented very poor conditioning. At first sight, this could seem in contradiction with the results presented by Nelson (2000,b), which verified that large condition numbers of matrix  $[A]$  worsen the inverse problem solution, leading to large deviations from the desired values. It will be shown later in this work that ill-conditioned problems are associated with the sensitivity of the solutions with respect to the noise in the input pressure field measurements.

In conclusion, through a series of results obtained with different measurement grid configurations, and different distances between the receiving array and the source, it could be shown that, differently from standard NAH, the ESM is capable of reconstructing the acoustic field regardless of the distance source/source/reconstructed plane and source/reconstructed plane when good quality experimental data is available.

### 3.3 ESM: perturbation added to data

In order to make the numerical analysis more representative, the effects of different levels of noise was simulated by adding random disturbances to the original pressure field, which was obtained analytically, and the robustness of ESM and NAH were evaluated and compared. For each frequency, a matrix  $[P_R]$  of random complex elements was generated. The ratio of the RMS value of matrix  $[P]$  to the RMS value of matrix  $[P_R]$ , is multiplied by a value of percentage,  $P_o$ , which gives the weight of disturbance,  $P_T$ . The matrix  $[P_{\text{noise}}]$ , obtained by the multiplication of  $P_T$  by  $[P_R]$ , is added to the matrix  $[P]$ , resulting in the hologram of measured pressure,  $[P_E]$ . This is the input hologram of the radiation model.

$$P_T = P_o \frac{\text{RMS}([P])}{\text{RMS}([P_R])} \quad \Rightarrow \quad [P_{\text{noise}}] = P_T \cdot [P_R] \quad \Rightarrow \quad [P_E] = [P] + [P_{\text{noise}}]$$

In this analysis, the 200-source model illustrated in Fig.(1) was utilized. The estimates were achieved for different percentages of added error,  $P_o$ , varying from 10% to 100%. In an analogous form, planes were reconstructed at  $z = 2\text{cm}$ ,  $z = 6\text{cm}$ , and  $z = 10\text{cm}$ . Fig.(6) shows a series of plots depicting the relative error for the four systems analyzed. In computing these results, the frequency was fixed at 400Hz.

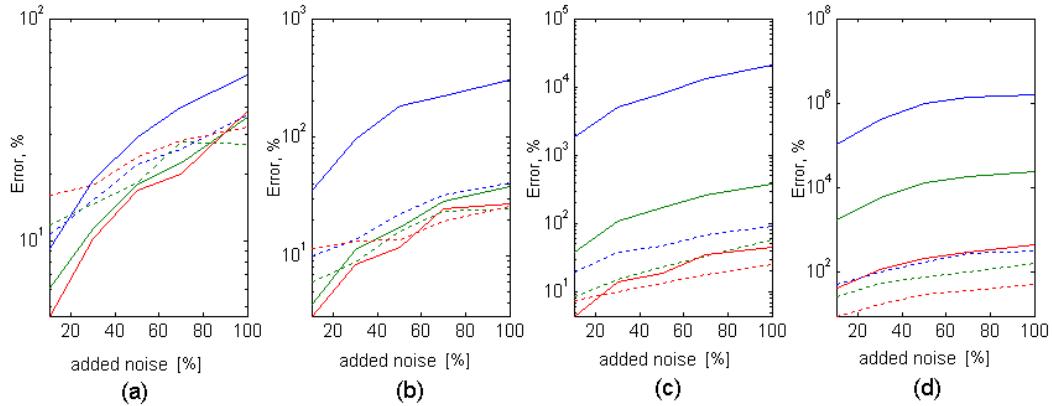


Figure 6. Relative error of ESM (solid) and NAH (dotted) results for three distances between the sources and the reconstruction plane at:  $z = 2\text{cm}$  (blue),  $z = 6\text{cm}$  (green) and  $z = 10\text{cm}$  (red),  $f = 400\text{ Hz}$ , for four distances between the receiving array and the source: (a)  $z_o = 1\text{cm}$ , (b)  $z_o = 4\text{cm}$ , (c)  $z_o = 8\text{cm}$ , and (d)  $z_o = 12\text{ cm}$ .

The error curves show that for the input plane very close to the source,  $z_o = 1\text{cm}$ , even in the presence of large noise levels, both methods presented similar results with good reconstruction, exhibiting a certain cancellation of the input disturbances in the projected field. For example, the introduction of 50% random error into the input measurement, yielded a relative error between 15% and 25%. As shown in Fig.(4), in this case, the ESM is well conditioned and, therefore, could obtain goods results. However, as the distance between the receiving array and the source increases, the solution leads to a noisy and erroneous reconstruction, and the NAH showed to be more robust. The reason why the ESM is no longer able to realize the reconstruction is the enlarged condition number of the matrix to be inverted, which affects the stability of the system, so that the solution becomes very sensitive to perturbations in the measured acoustic field.

Therefore, the results in Fig.(6) show that when the acquired data is polluted by noise, the ESM and NAH presented similar behavior when the receiving array is very close to the source. Moving the input plane away from the source, NAH showed to be a better method to obtain the radiated pressure field. However, for large distances, such as  $z_o = 12\text{cm}$ , both methods were not able to reconstruct the acoustic field.

#### 4. Experimental case

The experiment was performed on a plate mounted on a finite baffle. Full details of the work are presented in reference Pinho (2003). A steel plate 0.5m long, 0.4m wide and 0.0014m thick was used. It was mounted flush to a wood baffle 1.6m long, 1.4m wide, as shown in Fig.(7) and Fig.(8). The plate was excited by a shaker using a random noise signal. The experiment was undertaken in a semi anechoic room (dimensions 2.14m x 2.7m x 2.7m), which, according to Colinas (1999), simulates the free field for frequencies above 424 Hz.



Figure 7. The steel plate supported.



Figure 8. The plate mounted on a finite baffle.

The input force was measured using a force transducer and FRFs were obtained for a line grid of 15 microphones, spaced apart from one another by a distance  $dx = 0.029\text{m}$ . The microphone line grid was swept over the plate dimension in 21 lines of measurement, resulting in 315 discretization points of the pressure field. Holograms were obtained for two parallel planes on a surface of the same dimensions as

the plate. First, measurements were made the near field, at plane  $z_0 = 0.040\text{m}$  and, later, at plane  $z = 0.100\text{m}$ , in order yield data that could be used to validate the experimental result. In the measurements of the two holograms, a spacing distance of  $dy = 0.025\text{m}$  between the microphone lines was used.

In order to apply the NAH to compare with the ESM reconstruction, some aspects of the experimental setup were considered, such as: (1) the aperture,  $d = \max(dx, dy) = 0,029$ , gives the maximum frequency of analysis:  $f_{\max} = c / 2d \cong 5,9 \text{ kHz}$ , where  $c$  is the speed of sound in the medium; (2) measurement plane distance  $z_0$  should be contained in the sub-space:  $d \leq z_0 \leq 2d$ ; (3) due to the dimensions of the sensor grid utilized, the minimum frequency would be  $858 \text{ Hz}$ . However, using the regressive technique (RDFS), the NAH analysis can be extended to  $f_{\min} = 424 \text{ Hz}$ , which is the minimum frequency for which the semi anechoic room behaves like a free field.

In the ESM, a 315-source model was utilized, which, in previous analyses, yielded the best reconstruction results. The sources were distributed at plane  $z = 0$  in coordinates that are identical to the measurement grid.

Initially, in order to evaluate the ESM model utilizing the Tikhonov regularization tool, the regularization parameter,  $\beta$ , was determined for each frequency of analysis from the L-Curve method (Schuhmacher, 2000). Using the parameter  $\beta$  calculated, which is shown in Fig.(9), the regularization was applied and a regularized system was achieved. Fig.(10) depicts the comparison of the conditioning number curves for both systems.

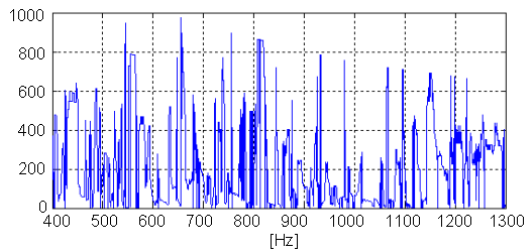


Figure 9. Regularization parameter  $\beta$ .

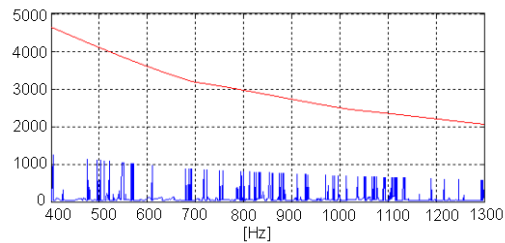


Figure 10 Conditioning number curve: regularized (blue) and not regularized (red)

From the curves shown in Fig(10), it can be clearly noticed that the Tikhonov regularization improves the conditioning number of the system. From the pressure data measured in the plane  $z_0 = 4\text{cm}$ , the pressure field in the plane  $z = 10 \text{ cm}$  was reconstructed. The relative error of the reconstruction estimated by the ESM, regularized and not-regularized, were compared in Fig(11).

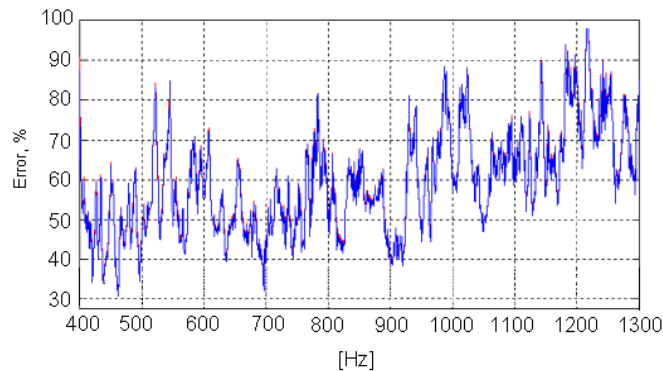


Figure 11. Relative error: regularized (blue) and not regularized (red).

By comparing the relative error curves shown in Fig.(11), no significant difference can be noticed and, therefore, the advantages of the Tikhonov regularization in the ESM method are not clear. Fig.(12) shows a series of reconstructed holograms where a qualitative analysis of the effects of the Tikhonov regularization could be performed.

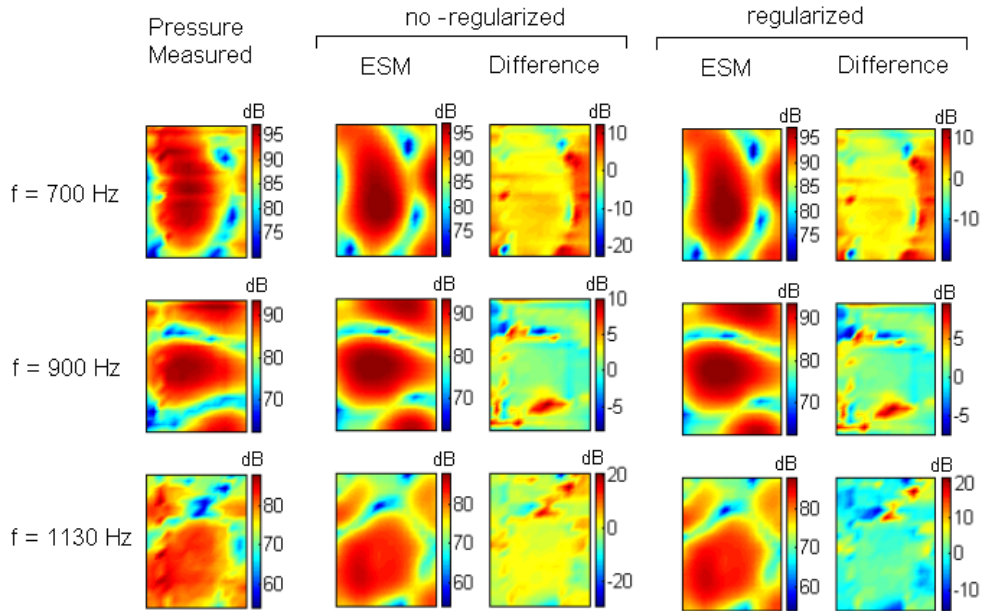


Figure 12. Experimental pressure field reconstructed by ESM at  $z = 10\text{cm}$ .

By comparing the results in Fig.(12), particularly the difference holograms, it can be noticed that the ESM associated with the Tikhonov regularization leads to more accurate solutions, where the regularization technique can be seen as a filter, which removes some peaks of noise from the estimated field. Moreover, it could be noted that, although the ESM solution has presented high values of relative error, as shown in Fig. (13), the method was able to reconstruct the acoustic field quite efficiently.

A comparative analysis between the two acoustical holography methods applied for the experimental case is shown in Fig(13). Here, the regularized ESM and the NAH with RDFS were used.

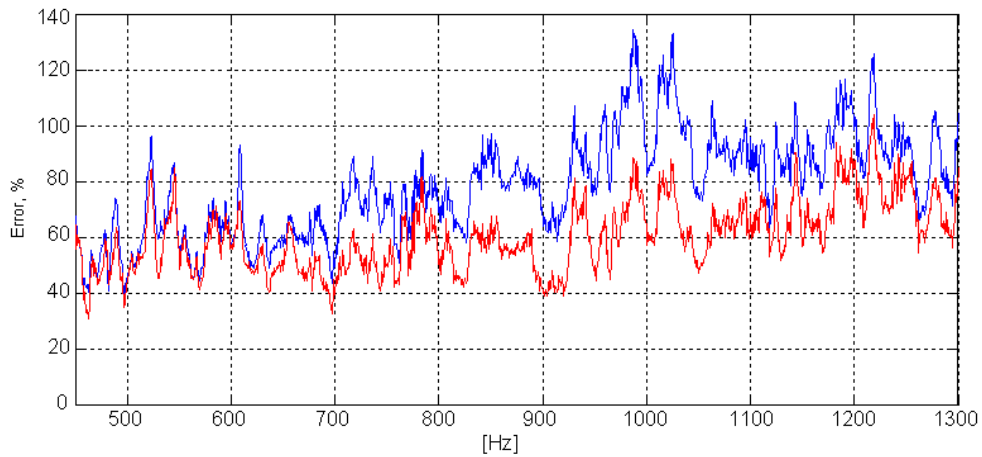


Figure 13. Relative error: ESM (red) and NAH (blue).

The error curves depicted in Fig.(13) allow us to compare the behavior of both methods. At low frequencies ( $f < 650\text{Hz}$ ), the two curves are very close. For higher frequencies, the ESM reconstruction, in general, leads to more accurate results, when compared with NAH. Furthermore, in order to obtain a qualitative assessment of the reconstructed fields by the two methods, Fig.(14) presents some pressure hologram estimates.

The pressure fields depicted in Fig.(14) ratify the previous conclusions, showing that the ESM results are quite accurate when compared with the NAH solution, in this case.

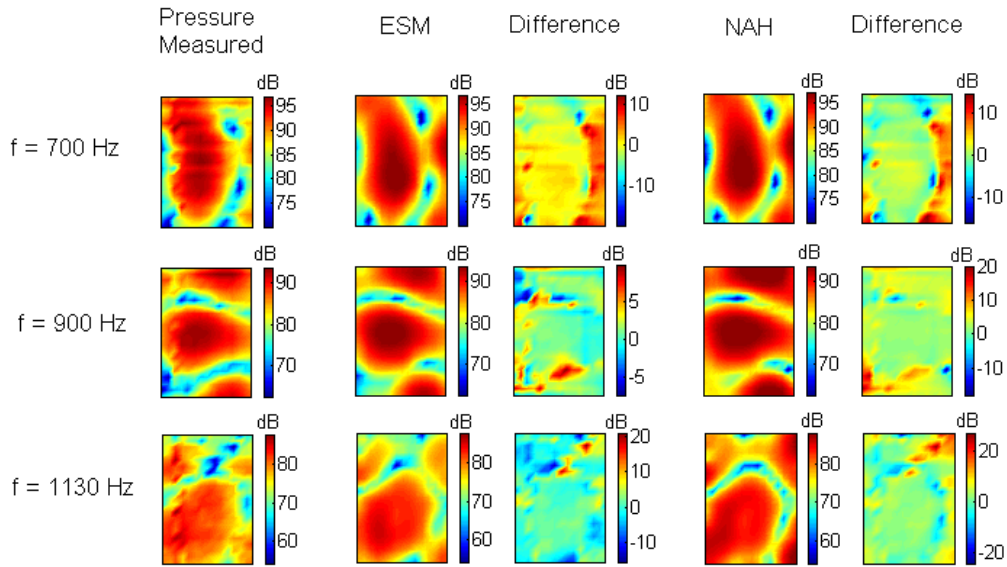


Figure 14. Experimental pressure field reconstructed in  $z = 10\text{cm}$  by ESM and NAH.

### 5. Other advantages of ESM

Once the strength of the modeled sources is determined, unlike in NAH, the ESM allows to estimate the vibroacoustic field independently of the dimensions of the measurement grid or the coordinate system utilized. To illustrate the importance of this characteristic, it is shown in Fig.(15) the sound field reconstructed in the plane  $z = 10\text{cm}$ , at frequency 590 Hz, where the black rectangle in the center of the figure indicates the plate position, where the pressure measurements were made.

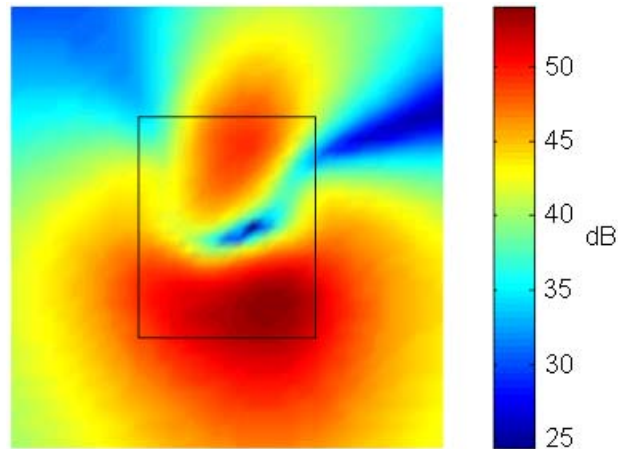


Figure 15. Experimental pressure field reconstructed by ESM for dimensions much larger than the plate, which is indicated by a black rectangle.

It can be observed that, in this case, a lot of information about the pressure field radiated would not be considered if just the sound field limited by the plate dimensions were analyzed. To show another important aspect of ESM, Fig.(16) presents the pressure field reconstructed on a spherical surface, for the frequency of 590 Hz.

In Fig.(16) illustrated the capability of the ESM to reconstruct the pressure field on any desired surface, with any coordinate system, independently of the coordinate system utilized in the measurement setup, resulting in a much larger flexibility in the acoustic reconstruction process when compared with NAH.

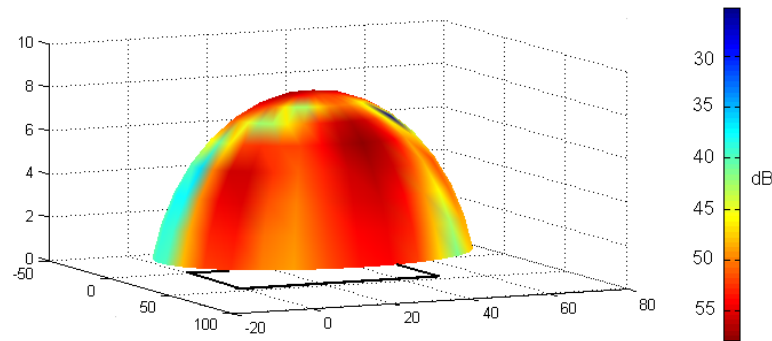


Figure 16. Pressure field estimated by ESM around the plate (indicated by a black rectangle) in a spherical coordinate system.

## 6. Conclusion

Differently from standard NAH, the ESM is capable of obtaining a good acoustic source reconstruction with little regard to either the distance source/ measurement plane or the distance source/reconstructed plane provided the measurement data is accurate and is not noisy. The conditioning of the problem, which is shown to be highly dependent on the number of modeled sources and on the distance between the measurement grid and the source, is shown to be related with the algebraic system solution stability. When the problem is poorly conditioned, techniques such as Tikhonov's regularization can be useful for improving the accuracy of the reconstruction. Unlike NAH, ESM is shown to be independent of the coordinate system and the measurement grid utilized. ESM can be applied when the pressure data are obtained by arbitrary measurement grids.

## 7. Acknowledgement

This work was supported by the DaimlerChrysler of Brazil.

## 8. References

- Pinho, M. E. V., *Holografia acústica usando modelo de fontes elementares*, Msc. dissertation, Department of Computational Mechanics, University of Campinas, UNICAMP, Campinas, 2003.
- Koopmann, G.H, Song, L., Fahline, J.B., A method for computing acoustic field based on the principle of wave superposition, *JASA* 86 (6), December 1989, pp 2433–2438.
- Nelson, P.A., Yoon, S.H., Estimation of acoustic source strength by inverse methods: part I, conditioning of the inverse problem, *Journal of Sound and Vibration*, 2000(b), 233(4), pp 643-668.
- Nelson, P.A., Yoon, S.H., Estimation of acoustic source strength by inverse methods: part II, experimental investigation of methods for choosing regularization parameters, *Journal of Sound and Vibration*, 2000(a), 233(4), pp 669-705.
- Schuhmacher, A., *Sound source reconstruction using inverse sound field calculations*, Ph.D. dissertation, Department of Acoustic Technology, Technical University of Denmark, report no 77, 2000, ISSN 1397-0547.
- Williams, E.G, *Fourier acoustics: sound radiation and nearfield acoustical holography*, Academic Press, London, UK, 1999.
- Arruda, J.R.F., Mas, P., Sas, P., Minimization of statistical and deterministic errors in nearfield acoustic source identification, *Proceedings of Inter-noise 1997* (3), pp1295-1300.
- Colinas, N. G., *Caracterização vibroacústica usando holografia acústica de campo próximo*, Msc. Dissertation, Department of Computational Mechanics, University of Campinas, UNICAMP, Campinas, 1999.
- Magalhães, M. B. S., *Intensidade supersônica e eficiência de radiação acústica em fontes de geometria arbitrária*, Dr. thesis, Mechanical engineering, COPPE/UFRJ, Rio de Janeiro, outubro de 2002.
- Barbosa, W. A., *Holografia acústica utilizando modelos de fontes elementares*, Dr. Thesis, Mechanical engineering, UFSC, Florianópolis, 2001.